PNAS
www.pnas.org

Supplementary Information for

Global impacts of recent Southern Ocean cooling

Sarah M. Kang*, Yue Yu, Clara Deser*, Xiyue Zhang, In-Sik Kang, Sun-Seon Lee, Keith B. Rodgers, and Paulo Ceppi

*Corresponding authors: Sarah M. Kang and Clara Deser

Email: skang@unist.ac.kr and cdeser@ucar.edu

This PDF file includes:

Figures S1 to S14

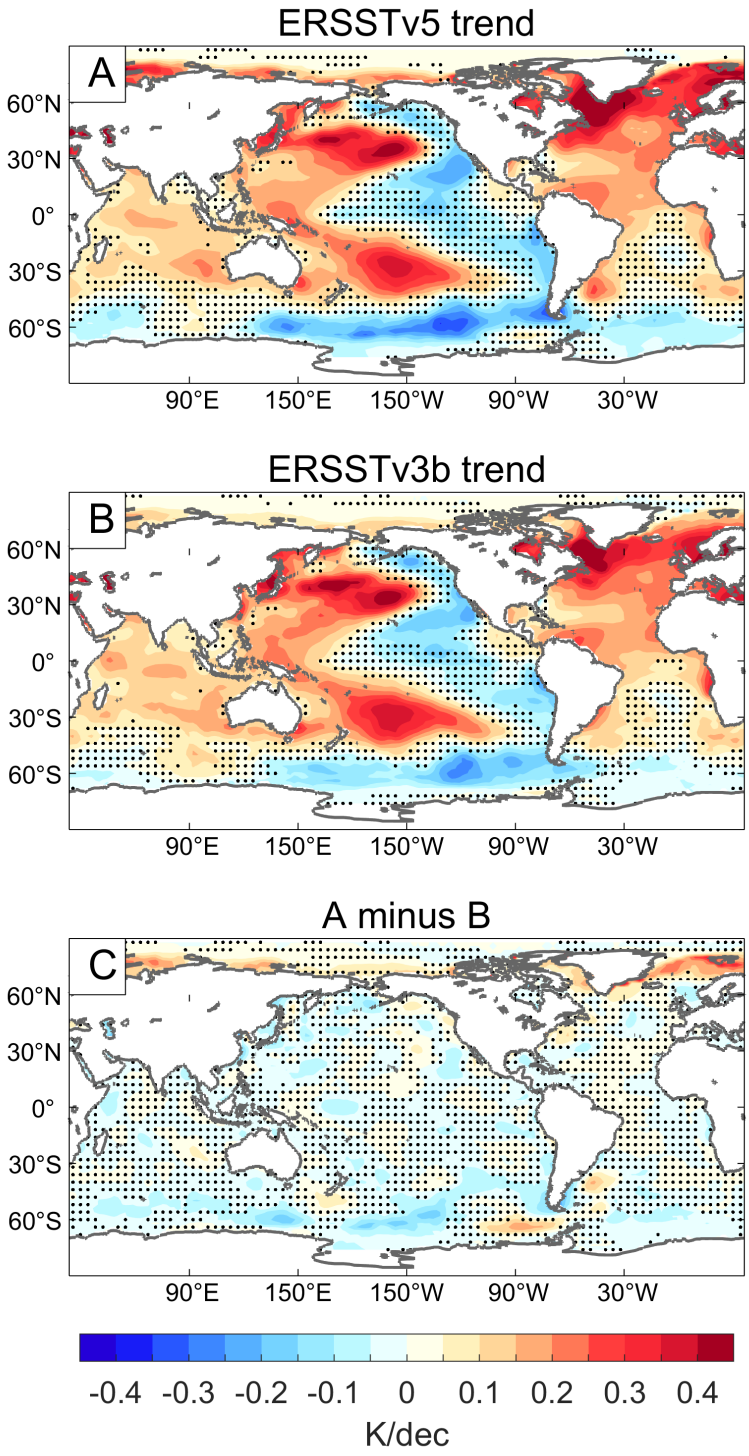

Fig. S1. Observed SST trends between 1979-2013. Observation dataset using (*A*) ERSSTv5 and (*B*) ERSSTv3b, and (*C*) the difference between ERSSTv5 and ERSSTv3b. Stippling indicates a local trend that is not statistically significant at 95% confidence level.

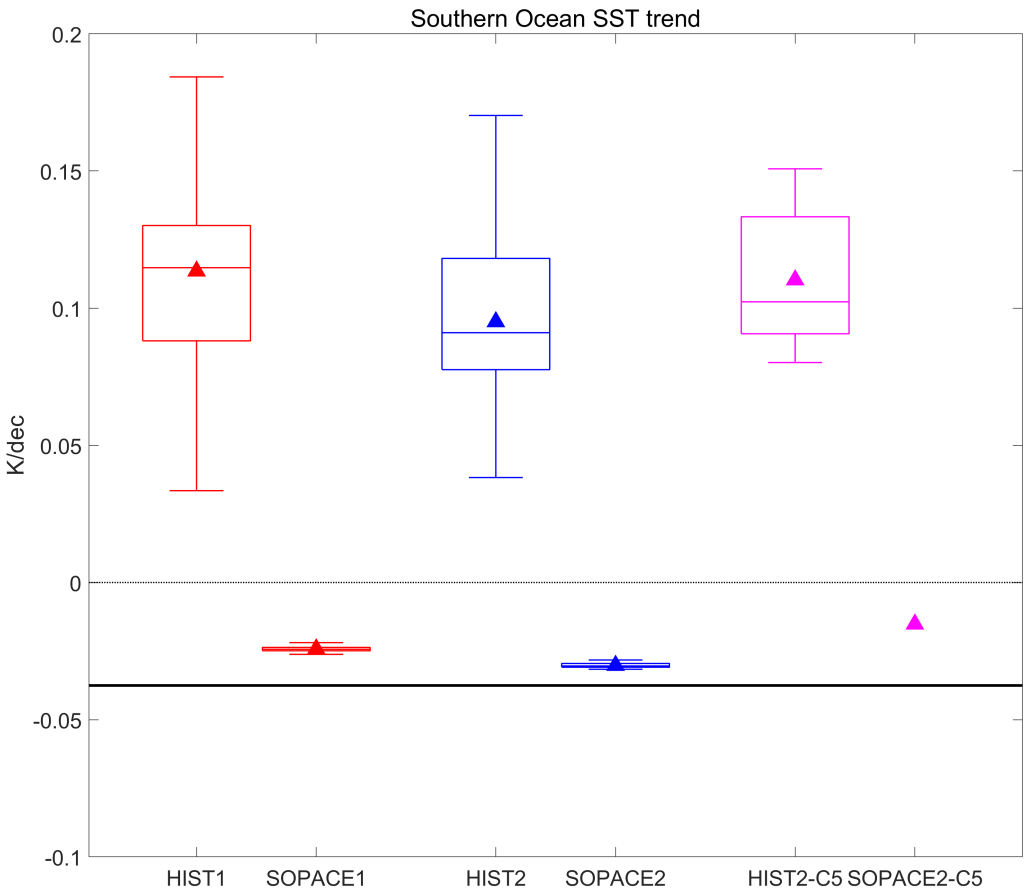

Fig. S2. Southern Ocean SST trends. Box-and-whisker plot of SST trends averaged between 70°S and 40°S. Black horizonal line shows the observed estimate from ERSSTv5. The SOPACE2-C5 value is obtained by subtracting SO-driven2 from [HIST2-C5].

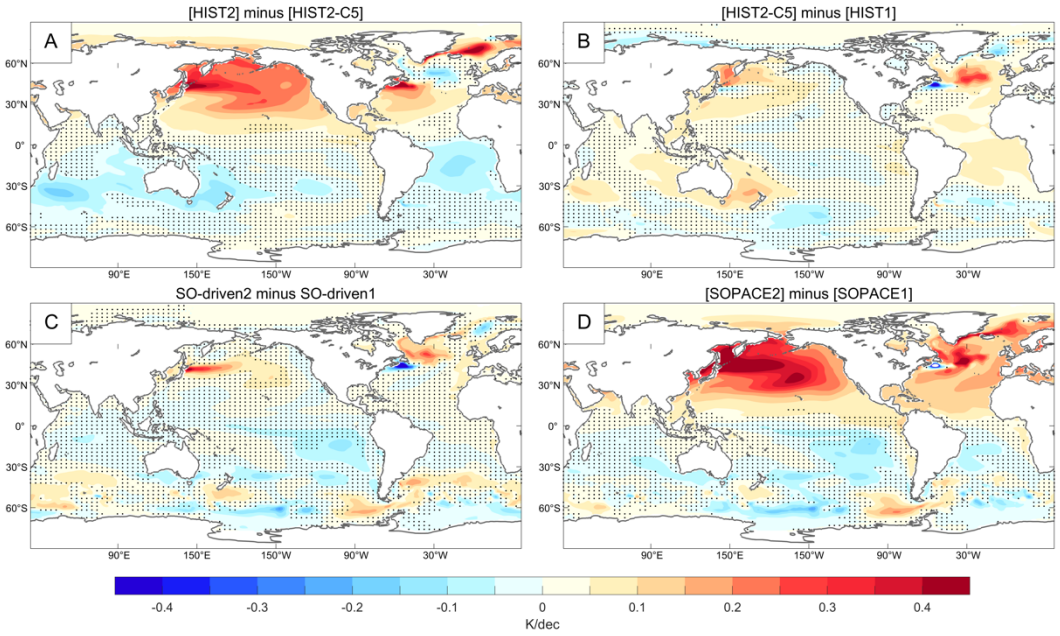

Fig. S3. Annual-mean SST trend differences between (*A*) [HIST2] and [HIST2-C5], representing forcing uncertainty, (*B*) [HIST2-C5] and [HIST1], representing model structural uncertainty, (*C*) SO-driven2 and SO-driven1, and (*D*) [SOPACE2] and [SOPACE1]. Stippling indicates the difference that is not statistically significant at 95% confidence level.

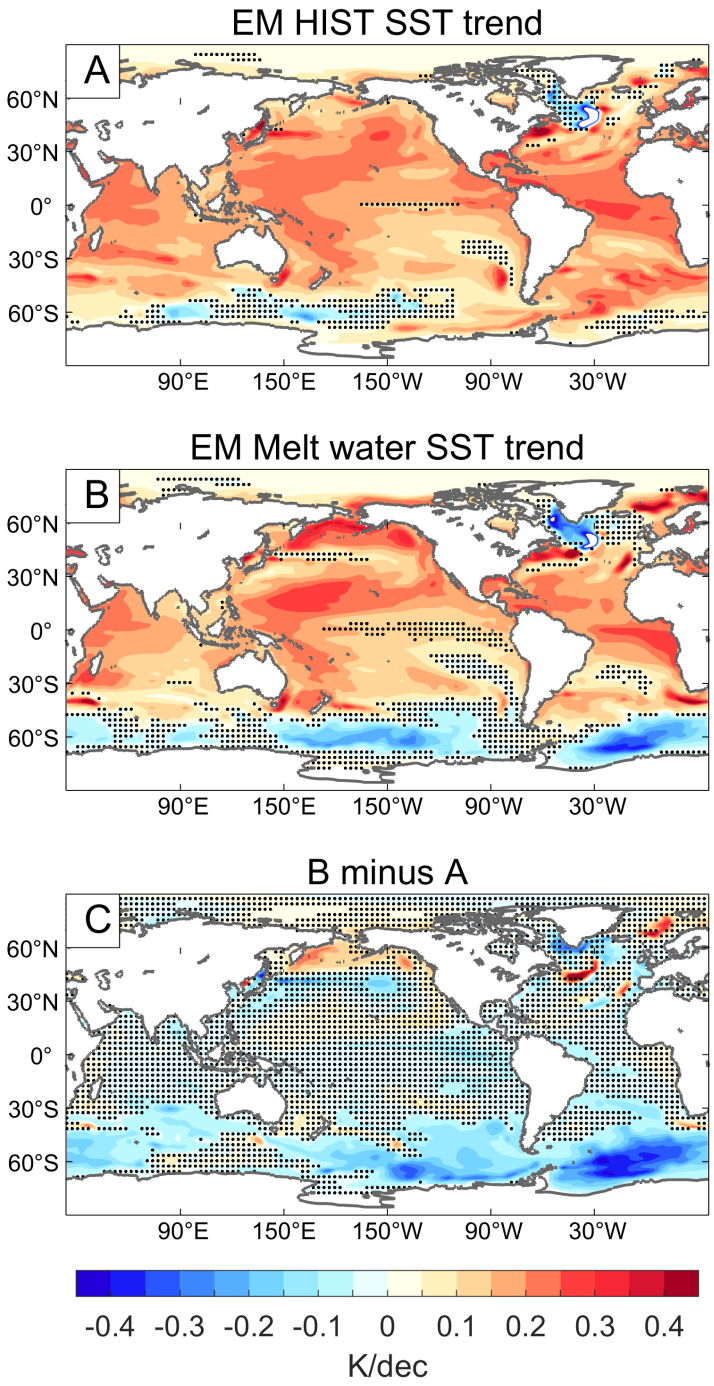

Fig. S4. Antarctic meltwater contribution. 6-member ensemble mean of global annual-mean SST trends between 1979-2013 in GFDL ESM2M under (*A*) CMIP5 historical scenario, (*B*) the same CMIP5 historical scenario but with added freshwater perturbation around the Antarctic coast. (*C*) Difference between (*B*) and (*A*), which quantifies the Antarctic meltwater contribution. Data from ref. (5). Stippling indicates a local trend that is not statistically significant at 95% confidence level.

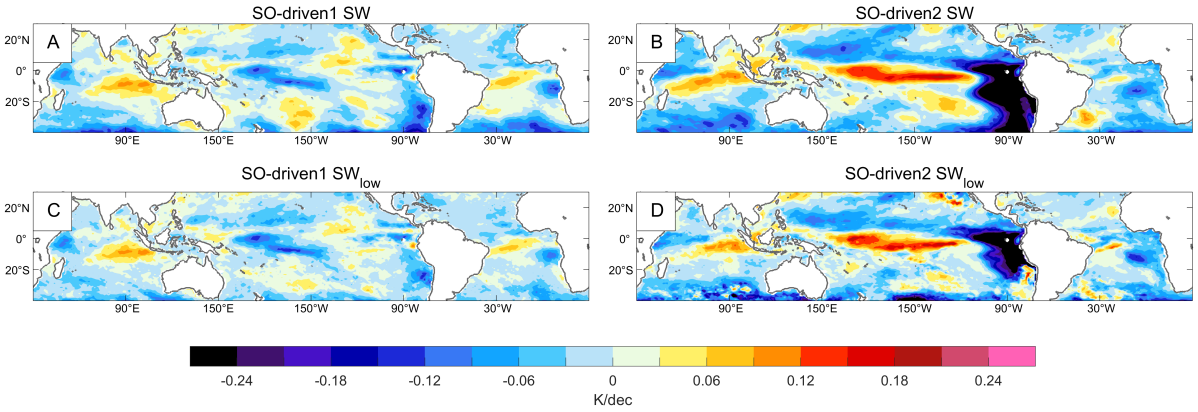

Fig. S5. Attribution of shortwave changes to low cloud changes. SST trend due to (*A*,*B*) shortwave flux changes, and (*C*,*D*) shortwave flux changes owing to low cloud changes, assuming that cloud radiative effects are dominated by low clouds when the absolute ratio of the longwave to shortwave cloud radiative effect is smaller than 0.41 (57), for SO-driven1 (left) and SO-driven2 (right). Similarity between the upper and lower panels indicates that the shortwave contribution is dominated by low cloud changes.

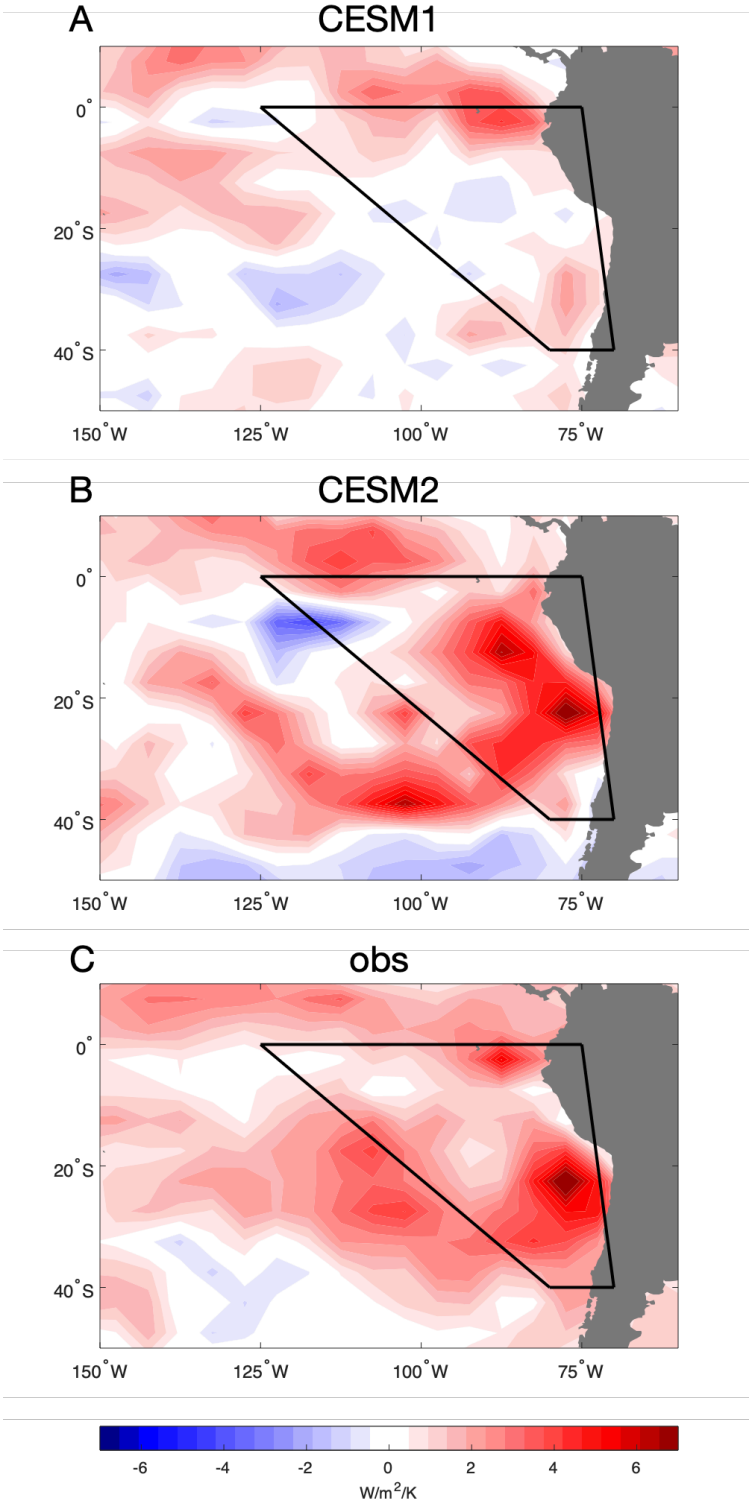

Fig. S6. Shortwave low-cloud sensitivity to SST in (*A*) CESM1, (*B*) CESM2, and (*C*) observations. See Materials and Methods for details.

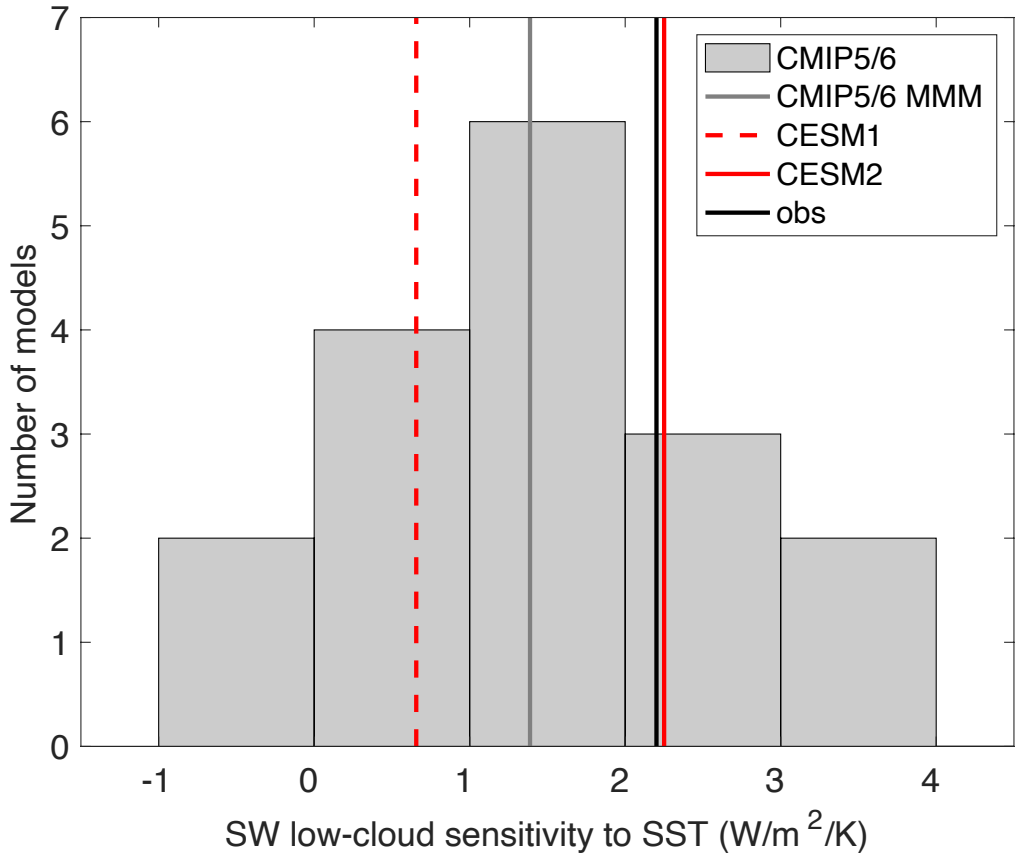

Fig. S7. Histogram of shortwave low-cloud sensitivity to SST averaged over the Southeast Pacific in 18 CMIP5/6 models, with the multi-model mean in a gray line, the CESM1 value in a red dashed line, the CESM2 value in a red solid line, and the observation estimates in a black solid line. See Materials and Methods for details.

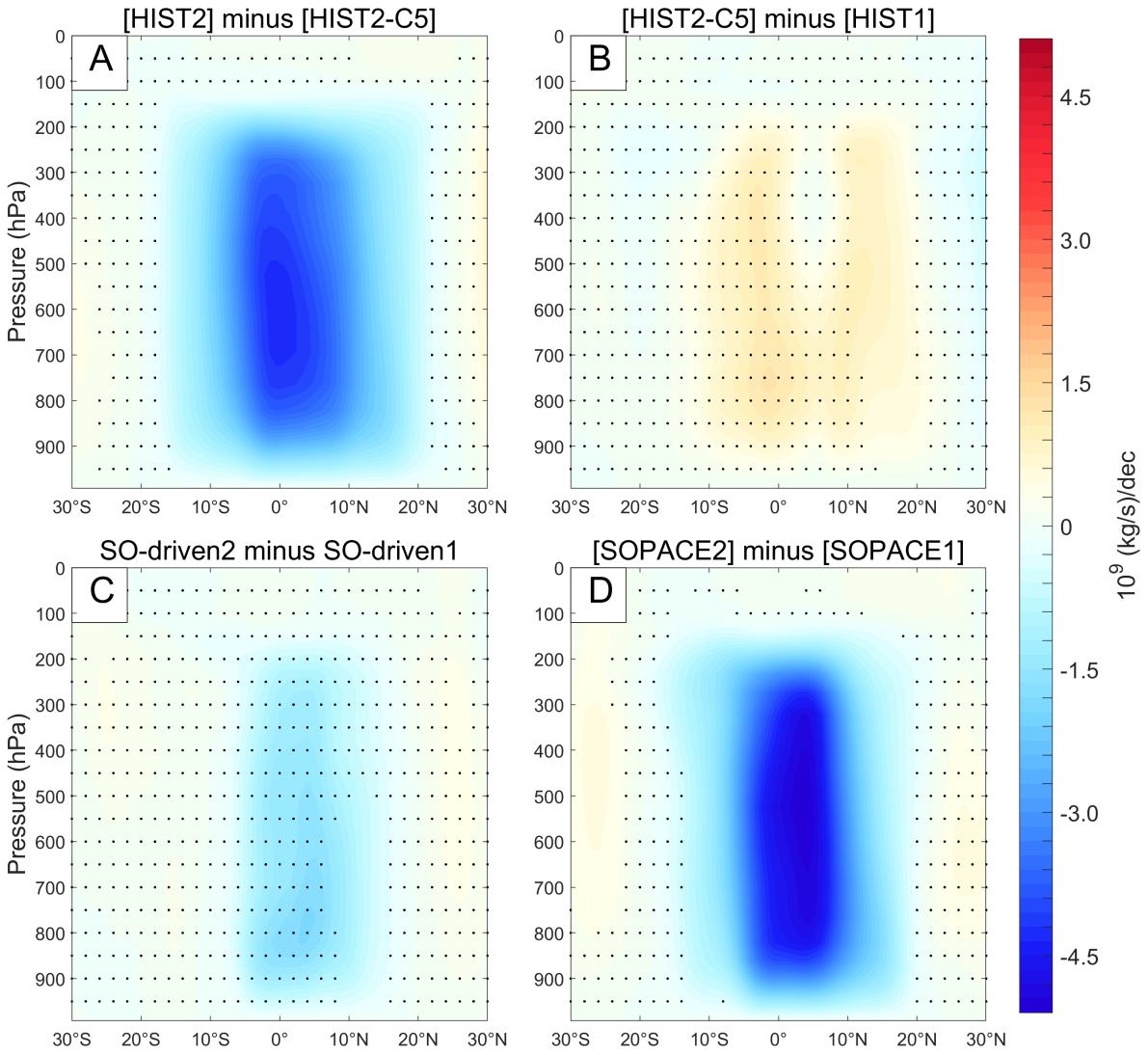

Fig. S8. Annual-mean trend differences in mean meridional streamfunction between (*A*) [HIST2] and [HIST2-C5], representing forcing uncertainty, (*B*) [HIST2-C5] and [HIST1], representing model structural uncertainty, (*C*) SO-driven2 and SO-driven1, and (*D*) [SOPACE2] and [SOPACE1]. Stippling indicates the difference that is not statistically significant at 95% confidence level.

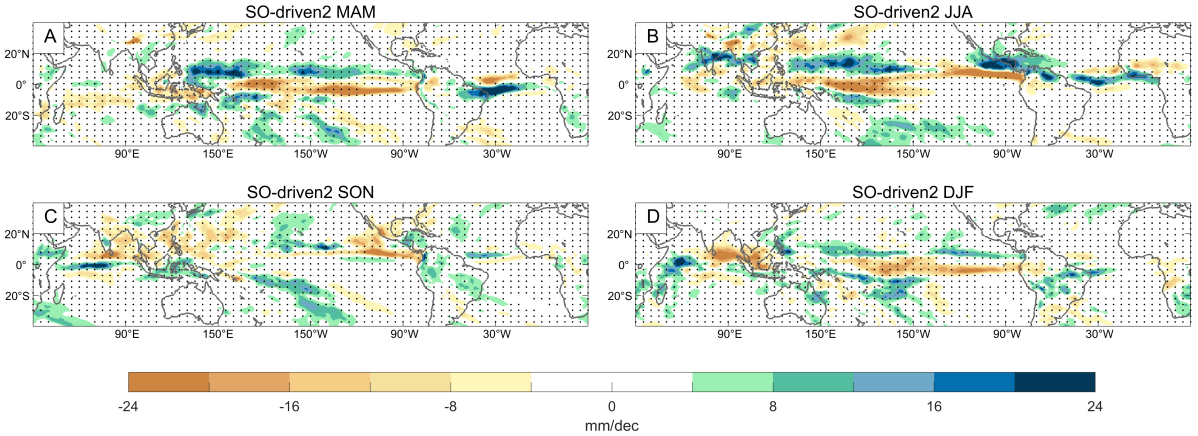

Fig. S9. Seasonal precipitation trends. Precipitation trends in SO-driven2 averaged over (*A*) March-April-May, (*B*) June-July-August, (*C*) September-October-November, and (*D*) December-January-February. Stippling indicates a local trend that is not statistically significant at 95% confidence level.

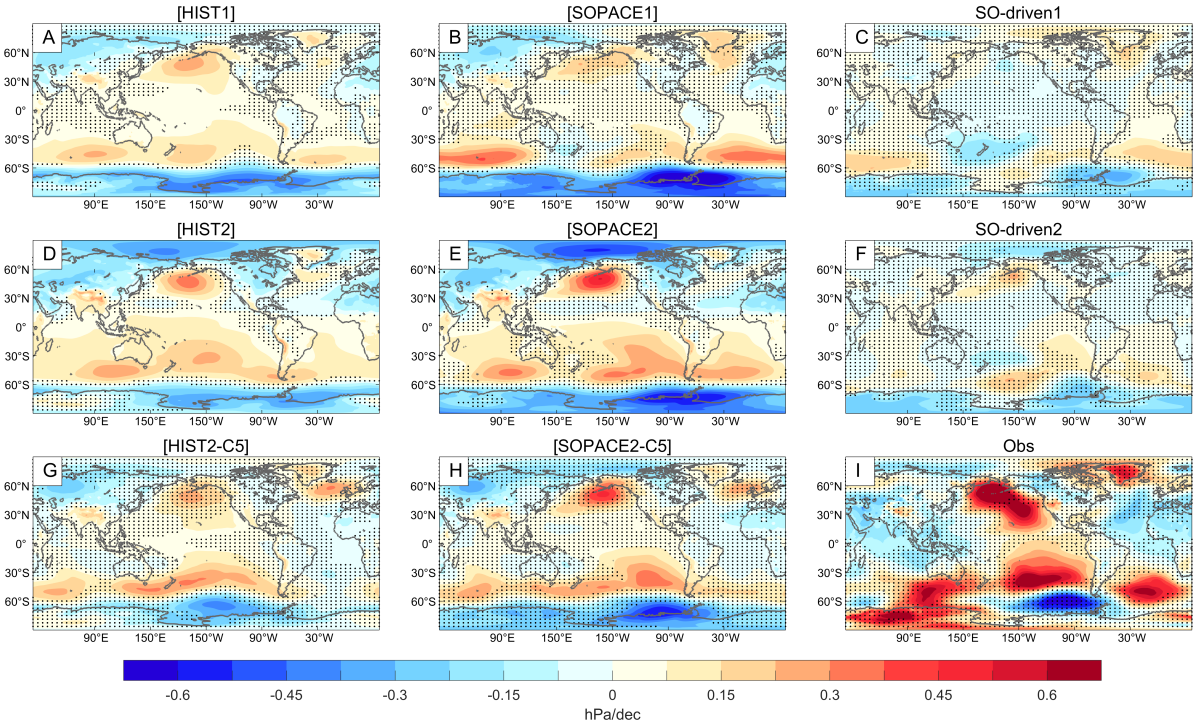

Fig. S10. Global sea level pressure trend maps. Annual-mean sea level pressure trends between 1979-2013 in (*A*) [HIST1], (*B*) [SOPACE1], (*C*) SO-driven1, (*D*) [HIST2], (*E*) [SOPACE2], (*F*) SO-driven2, (*G*) [HIST2-C5], (*H*) [SOPACE2-C5], and (*I*) ERA5 reanalysis (52). Stippling indicates a local trend that is not statistically significant at 95% confidence level.

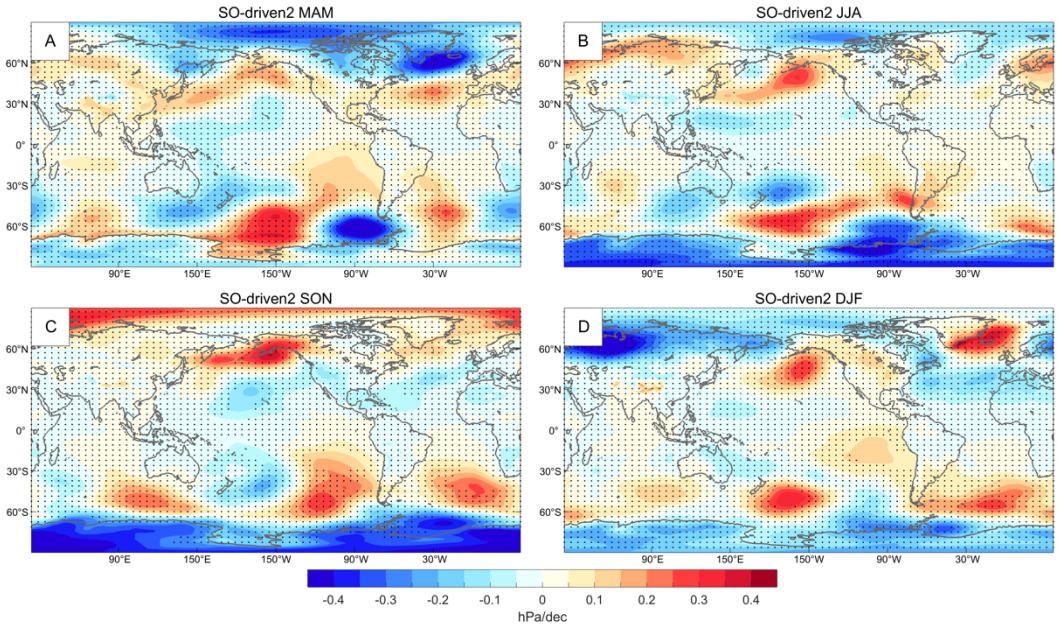

Fig. S11. Seasonal sea level pressure trends. Sea level pressure trends in SO-driven2 averaged over (*A*) March-April-May, (*B*) June-July-August, (*C*) September-October-November, and (*D*) December-January-February. Stippling indicates a local trend that is not statistically significant at 95% confidence level.

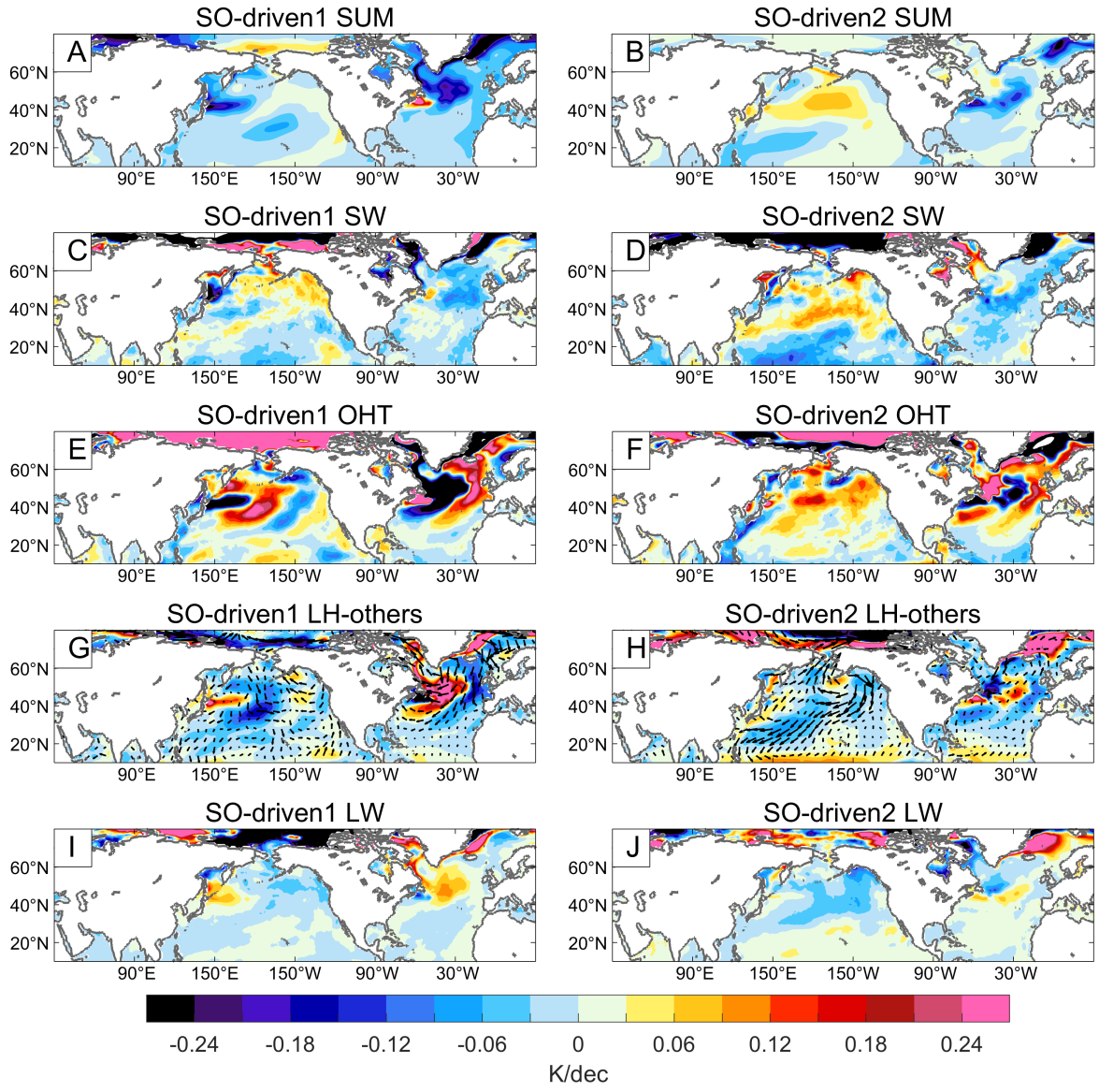

Fig. S12. SST trend decomposition via surface energy budget. Same as Fig. 3 but for a domain between 10°N and 80°N.

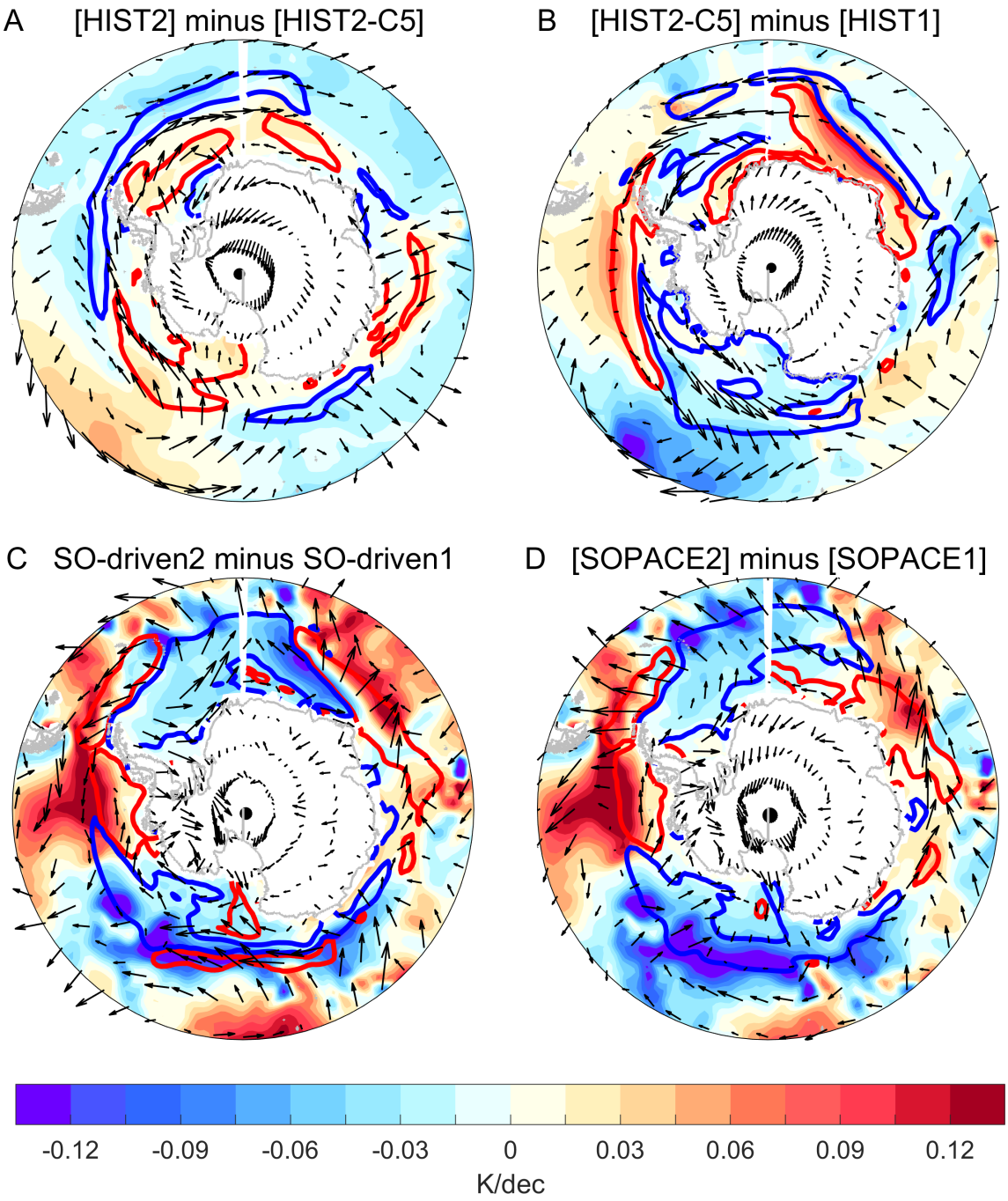

Fig. S13. Antarctic sea-ice and SST trends. Same as Fig. 6 but for the difference between (*A*) [HIST2] and [HIST2-C5], representing forcing uncertainty, (B) [HIST2-C5] and [HIST1], representing model structural uncertainty, (*C*) SO-driven2 and SO-driven1, and (*D*) [SOPACE2] and [SOPACE1].

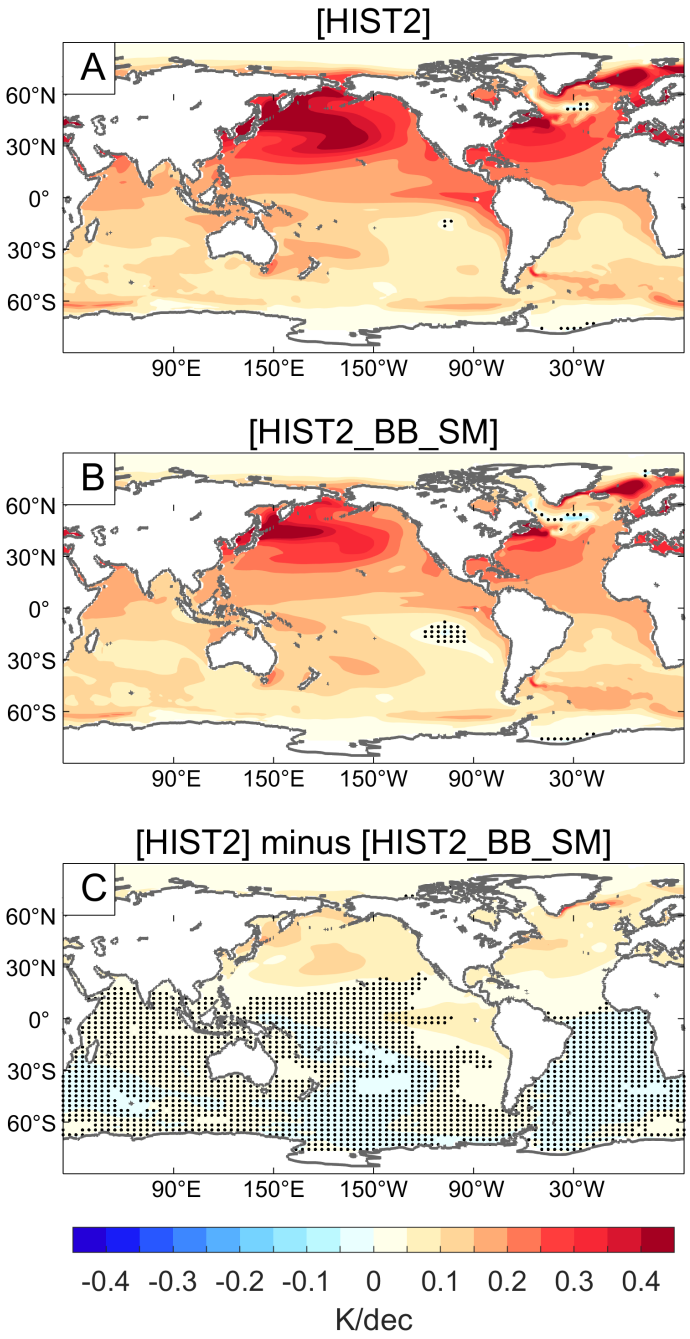

Fig. S14. Role of different biomass burning aerosol emissions. Ensemble mean of global annual-mean SST trends between 1979-2013 in (*A*) HIST2 (i.e., the first 50 members of CESM2 large-ensemble simulations forced by CMIP6 historical radiative forcing), (*B*) HIST2_BB_SM (i.e., 40 members of CESM2 large-ensemble simulations forced by CMIP6 historical radiative forcing with the biomass burning emissions smoothed in time), and (*C*) difference between (*B*) and (*A*). Stippling indicates a local trend that is not statistically significant at 95% confidence level.